Acta Oceanol. Sin., 2025, Vol. 44, No. 4, P. 75–89
https://doi.org/10.1007/s13131-025-2480-6

Monthly variations in nutrient utilization along 45°E transect in the Cosmonaut Sea, East Antarctica during austral summer

Xufeng Yang[1], Dong Li[1], Jun Zhao[1*], Cai Zhang[1], Changfeng Zhu[1], Shunan Cao[2], Guangfu Luo[2], Gaojing Fan[2], Yongming Sun[3], Ji Hu[1], Haifeng Zhang[1], Peisong Yu[1], Weiping Sun[1], Jianming Pan[1], Jianfeng He[2]

[1] Key Laboratory of Marine Ecosystem Dynamics, Second Institute of Oceanography, Ministry of Natural Resources, Hangzhou 310012, China
[2] Polar Research Institute of China, Ministry of Natural Resources, Shanghai 200136, China
[3] Key Laboratory of Physical Oceanography of Ministry of Education, Ocean University of China, Qingdao 266100, China

Received 14 October 2024; accepted 23 April 2025
© Chinese Society for Oceanography and Springer-Verlag GmbH Germany, part of Springer Nature 2025

Abstract
Nutrient uptake status dominates phytoplankton biomass and community structure in the Southern Ocean during austral summer, yet how nutrient utilization variability responds to phytoplankton community succession is still unclear, partly due to lack of data spanning the entire summer. In this study, nitrate, phosphate, and silicate combined with temperature, salinity, and apparent oxygen utilization (AOU) were analyzed along 45°E in the Cosmonaut Sea during December 2019, January 2021, and February 2022. The variations in nutrient utilization in the euphotic layer were studied using biogeochemical tracers, and seasonal nutrient depletion was also estimated. The results showed that nutrient distribution varied significantly from December to February. Significant positive correlations were observed for nitrate and silicate concentrations with salinity and AOU, indicating that nutrient distributions were mainly influenced by water mass and phytoplankton production. Increasing $\Delta[N^*]$ and decreasing $\Delta[Si^*]$ in the upper 50 m were observed south of 63.5°S from December to February, which possibly contributed to a progressive shift in dominant phytoplankton population from *Phaeocystis antarctica* to diatoms. The seasonal nutrient depletion generally increased from December to February. Moreover, the consumption of silicate substantially increased compared to nitrate, indicating that the abundance of diatoms was increasing with time during the austral summer. Our observations suggest that nutrient utilization status is closely related to phytoplankton community structure in the euphotic layer of the Cosmonaut Sea.

Key words nutrient, biogeochemical tracers, seasonal depletion, monthly variation, Cosmonaut Sea

Citation Yang Xufeng, Li Dong, Zhao Jun, Zhang Cai, Zhu Changfeng, Cao Shunan, Luo Guangfu, Fan Gaojing, Sun Yongming, Hu Ji, Zhang Haifeng, Yu Peisong, Sun Weiping, Pan Jianming, He Jianfeng. 2025. Monthly variations in nutrient utilization along 45°E transect in the Cosmonaut Sea, East Antarctica during austral summer. Acta Oceanologica Sinica, 44(4): 75–89, doi: 10.1007/s13131-025-2480-6

1 Introduction

Dissolved nutrient is fundamental to sustaining ocean life growth, thus its distribution within the euphotic layer plays an important role in the distribution of phytoplankton and other ocean life and vice versa (Sarmiento, 2004). The supply amount and structure of nutrients have a significant effect on phytoplankton biomass and community structure (Quigg et al., 2003). The nutrient uptakes of various phytoplankton species are also obviously different,

Foundation item: The National Polar Special Program "Impact and Response of Antarctic Seas to Climate Change" under contract Nos IRASCC 01-01-02 and IRASCC 02-02; the National Key Research and Development Program of China under contract No. 2022YFE0136500; the National Natural Science Foundation of China (NSFC) under contract Nos 41976228, 42276255 and 42176227; the Scientific Research Fund of the Second Institute of Oceanography under contract Nos JG2011, JG2211 and JG2013.
*Corresponding author, E-mail: jzhao@sio.org.cn

thus changing the nutrient stock and structure in the euphotic depths. Phytoplankton usually assimilates dissolved nutrients in a similar ratio called canonical Redfield's N:P:Si of 16:1:16, which leads to the same nutrient ratio for phytoplankton biomass. The above rule is very helpful for researchers to understand the ocean biogeochemical cycle and phytoplankton community shift in the euphotic layer. Without a doubt, various N:P:Si ratios are also observed in some sea areas, especially in the Southern Ocean (Martiny et al., 2013), which shows that nutrient consumption deviates from conventional ratios, possibly due to special phytoplankton community structure.

The Southern Ocean is a huge carbon sink region due to carbon fixation by phytoplankton and its cold environment (Gruber et al., 2019a, b). Nitrogen, phosphorus, and silicon are not the limiting factors for primary production in the Southern Ocean, which is characterized by high nutrient and low chlorophyll (HNLC) compared to the other oceans. Even though the coastal area near the ice shelf sometimes shows high production, the phenomenon lasts for a short time (Rubin et al., 2004). Light limitation (Mitchell et al., 1991; Fan et al., 2024), unstable water column (Nelson et al., 1991), deficiency of micronutrients such as Fe (Buma et al., 1991; Holm-Hansen et al., 1994), zooplankton grazing (Burkill et al., 1955), and other factors can lead to high nutrient and low production. The researches show that Fe limitation can induce the change of N:P:Si uptake ratio by phytoplankton and further regulate the nutrient cycle in the Southern Ocean (Hutchins et al., 1998; Takeda et al., 1998). The ongoing research on nutrient status will help us discover the mechanism of low production in the Southern Ocean.

$\Delta[N^*]$ ($NO_3^- - 16PO_4^{3-}$) and $\Delta[Si^*]$ ($SiO_3^{2-} - NO_3^-$), two biogeochemical tracers, were proposed to evaluate the difference between nutrient supply and phytoplankton uptake (Sarmiento et al., 2004; Parli et al., 2020), which can further reflect phytoplankton dominant species. For example, a decrease in $\Delta[Si^*]$ indicates increasing siliceous-shell phytoplankton in the community due to increasing silicate consumption. Parli et al. (2020) found that most of the tracer distributions can be explained by the dominant phytoplankton populations. Thus, $\Delta[N^*]$ and $\Delta[Si^*]$ are useful tools to understand the interactive relationship between nutrient cycles and phytoplankton production.

Several studies have been carried out on nutrient distribution (Westwood et al., 2010; Huang et al., 2022), tracer ($\Delta[N^*]$ and $\Delta[Si^*]$) variability (Parli et al., 2020), nitrogen uptake rates (Gandhi et al., 2012), and seasonal nutrient depletion (Parli et al., 2020) in the Cosmonaut Sea during the austral summer, the highest productive season, which help us understand the nutrient status at a certain period of summer. It is a pity that the results are photographic, so we cannot comprehensively understand how nutrient distribution, structure, and consumption change with time during the entire summer. In this study, based on the 36 th, 37 th, and 38 th China Antarctic Research Expedition (CHINARE), we studied a typical section covering the coastal area and open ocean in the Cosmonaut Sea. The most important thing was that sampling time covered the entire summer, including early summer (December), mid-summer (January), and late summer (February). The characteristics of nutrient distribution, biogeochemical tracers ($\Delta[N^*]$ and $\Delta[Si^*]$), and nutrient depletion during each month were analyzed to discuss the nutrient variability and how phytoplankton biomass and community structure responded to nutrient change from early summer to later summer.

2 Materials and methods

2.1 *Study area and oceanography*

The study area is located along 45°E between 62°S and 68°S in the Cosmonaut Sea, East Antarctica (Fig. 1). There are three main circulations existing in the region, including the Weddell Gyre (WG), the southern boundary (SB) of the Antarctic circumpolar current, and the Antarctic slope current (ASC) (Fig. 1). The southern extent of circumpolar deep water (CDW) is described by Orsi et al. (1995) as SB. Warm and high-nutrient CDW is covered by Antarctic surface water, and thus its upwelling or intrusion can lead to the increase of upper nutrient concentrations (Huang et al., 2022). The WG, the dominant circulation located in the western part of 40°E in the Cosmonaut Sea, causes a shallower, warmer, and fresher seasonal mixed layer in the western region than those of the eastern region (Williams et al., 2010). The modified circumpolar deep water (MCDW) in the study area is notably warmer and saltier than those in areas further east (Qi et al., 2025). As for the eastern part of the Cosmonaut Sea, the influence from WG shows a meridional decrease. In addition, the ASC with a robust narrow westward-flowing jet brings fresh shelf water, including bioavailable iron, and causes high chlorophyll *a* concentration along the shore (Meijers et al., 2010).

The upper water column is dominated by Antarctic surface water (AASW) and winter water (WW), mainly characterized by lower salinity and lower temperature (Qi et al. 2025). Below 200 m, saline and warm CDW prevails. Sea ice meltwater (SIW) is mainly distributed within the upper 100 m near the shelf. The masses and circulations, characterized by the special physicochemical environment, are the key factors to nutrient distribution in the top 250 m of the water column (Orsi et al., 1995).

2.2 *Sample collection and measurements*

The sampling was conducted in the Cosmonaut Sea aboard R/V *Xuelong 2* from December 24, 2019, to December 26, 2019; from January 16, 2021, to January 22, 2021; and from February 2, 2022, to February 14, 2022, during CHINARE-36, CHINARE-37, and CHINARE-38, separately. Considering that the sampling interval of each cruise is only one year, and meanwhile, there are no spe-

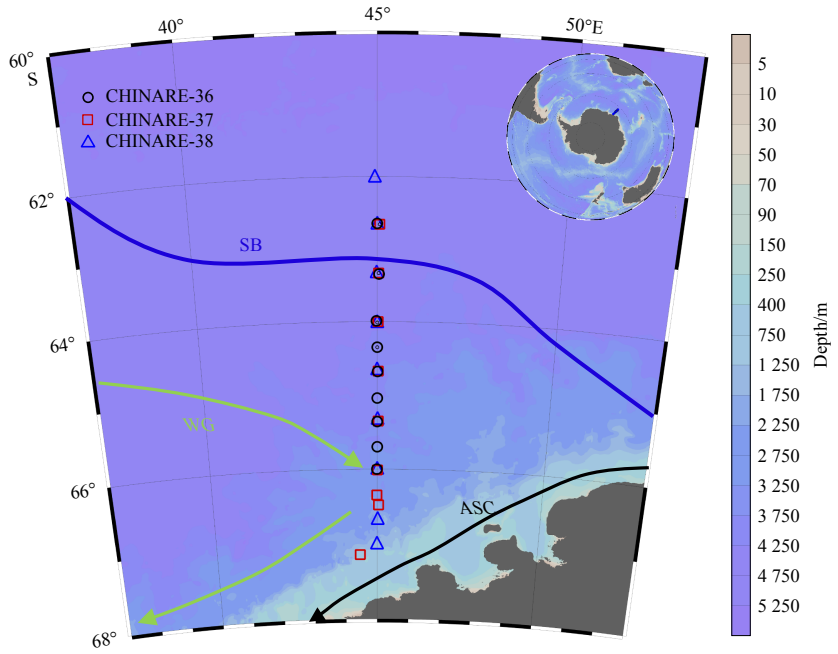


Fig. 1. Sampling stations of each cruise, bathymetry and circulation located in the Cosmonaut Sea. The black cycles, red squares and blue triangles indicate the sampling stations from the CHINARE-36, CHINARE-37 and CHINARE-38, respectively. The currents in the study area mainly include the southern boundary (SB) of the upper circumpolar deep water (blue line), the eastern boundary of Weddell Gyre (WG, cyan line) and Antarctic slope current (ASC, black line).

cial climate events occurring in the Cosmonaut Sea in recent years (Hao et al., 2025), inter-annual variations of some physical and biochemical parameters can be ignorable. Moreover, as an important influence factor on the biogeochemical cycle in this area, the sea ice concentration always decreases with time from December to February in each year, inferred from public sea ice concentration data from the university of Bremen (https://data.seaice.uni-bremen.de/databrowser/). Therefore, it was practicable to conduct the research on monthly nutrient variability using the data from the three cruises.

Discrete seawater samples from about 10 stations in each cruise were collected from 7 depths (0 m, 25 m, 50 m, 75 m, 100 m, 150 m and 200 m) using a Niskin sampler (5 L or 10 L) attached to a rosette connected to a Seabird 911plus CTD (Seabird, USA). Note that the samples from 150 m are missing during the CHINARE-36.

Temperature and salinity data were obtained from the Seabird 911plus CTD during CHINARE-37 and CHINARE-38. For the CHINARE-36, temperature and salinity data are from a moving vessel profiler.

The collected seawater samples were filtered with a 0.45 μm cellulose acetate filter membrane (Whatman, USA). The filtrate was collected in an acid-cleaned polypropylene bottle and stored in a −20℃ condition for nutrient measurement in the lab. The nitrate (NO_3^--N), phosphate (PO_4^{3-}-P), and silicate (SiO_3^{2-}-Si) concentrations were determined using the diazo method with a copper-cadmium reduction column, the phosphomolybdenum blue method, and the silicon-molybdenum blue method, respectively, by an AA3 automatic nutrient analyzer (SEAL, Germany). The nutrient concentrations of seawater samples were calculated by the linear relation between the standard solutions and their light absorption values. The standard solutions (GBW 08617-08645) used in the experiment were produced by the Marine Reference Material Center, Second Institute of Oceanography, Ministry of Natural Resources of China. The measurement precisions of nitrate, phosphate, and silicate are 0.06 μmol/L, 0.012 μmol/L and 0.05 μmol/L, respectively. Dissolved oxygen samples were collected in DO bottles, fixed with Winkler's reagents, acidified, and analyzed onboard by titrating against sodium thiosulphate. The dissolved oxygen concentrations were further used to calculate the apparent oxygen utilization (AOU). The above data were given detailedly in Table S1.

2.3 *The estimate of seasonal nutrient depletion*

Several research studies showed that phytoplankton consumed nutrients without the canonical Redfield's N:P:Si ratio of 16:1:16 (Hutchins et al., 1998; Timmermans et al., 2004; Giddy et al., 2012; Martiny et al., 2013), especially in the Southern Ocean, which is indicative of an imbalance between nutrient supply and phytoplankton uptake. To further understand the observed differences between nutrient utilization and stoichiometry, two biogeochemical traces called $\Delta[N^*]$ and $\Delta[Si^*]$were introduced as important indicators of nutrient condition related to phytoplankton requirements (Sarmiento et al., 2004). The biogeochemical tracers were computed as follows:

$$\Delta[N^*] = [NO_3^-] - 16[PO_4^{3-}], \quad (1)$$

$$\Delta[\mathrm{Si}^*] = [\mathrm{SiO}_3^{2-}] - [\mathrm{NO}_3^-]. \quad (2)$$

Seasonal nutrient depletion was estimated using the widely recognized $T_{\min}$ method given by Rubin et al. (2004). As a thermos-halocline will form in the Cosmonaut Sea during summer, the condition meets the basic principles of using the $T_{\min}$ method. Assuming that nutrient is mainly consumed by phytoplankton from spring due to the melting of sea ice and increasing light availability, nutrient depletion is estimated as the difference between observed nutrient stock and residual WW nutrient stock and can be calculated by integrating the water column from the surface to the depth of winter water. The expression is as follows:

$$\mathrm{NXU} = \int_0^z \Delta C \mathrm{d}z = \int_0^z (C_{\mathrm{ww}} - C_{\mathrm{sample}}) \mathrm{d}z, \quad (3)$$

where the seasonal nutrient depletion is expressed by the NXU. The character X in Eq. (3) represents nitrate, phosphate, or silicate. The character C denotes the nutrient concentration, and Z is for the water depth where the lowest temperature is located. The depth of winter water in the study area was 50 m or 75 m.

3 Results

3.1 *Basic hydrological parameters*

The vertical distributions of temperature and salinity along the 45°E transect in the Cosmonaut Sea during December 2019 (Fig. 2a), January 2021 (Fig. 2b), and February 2022 (Fig. 2c) of the austral summer were illustrated in Fig. 2. Seawater temperatures ranged from −1.820℃ to 1.619℃ with an average value of (−0.637 ± 1.107)℃ in December. Similarly, the temperature varied from −1.838℃ to 1.601℃ with an average value of (−0.676 ± 1.177)℃ in January; however, it obviously rose in February, ranging from −1.838℃ to 1.737℃ with an average value of (0.101 ± 1.260)℃. Note that the temperatures of three stations at high-latitude regions were not collected in December, resulting in a slightly higher average temperature. Based on data from the same stations and depths, seawater temperatures showed a gradual increase from December to February, mostly resulting from the heating of the mixing layer. Vertically, seawater temperatures initially decreased with depth before increasing again below about 75 m during all three months, indicating the presence of a low-temperature layer, likely due to residual winter water. Additionally, higher latitudes exhibited lower seawater temperatures during all the months, especially in January. From December to February, the low-temperature zone located at high latitudes expanded northward, eventually being overtaken by intrusion of higher-temperature deep water from low latitudes.

As shown in Fig. 2, seawater salinity ranged from 33.616 to 34.693, with an average value of 34.186 ± 0.289 in December, whereas it displayed a wider range of 32.042 to 34.674, with an average of 34.088 ± 0.475 in January. In February, salinity ranged from 33.220 to 34.684, with an average value of 34.166 ± 0.385. Vertically, salinity increased with depth uniformly during December. As for January, the salinity of shallow water at high latitudes experienced a notable reduction, likely due to melting ice with low salinity, while deep-water salinity slightly decreased. In February, the areas of low salinity

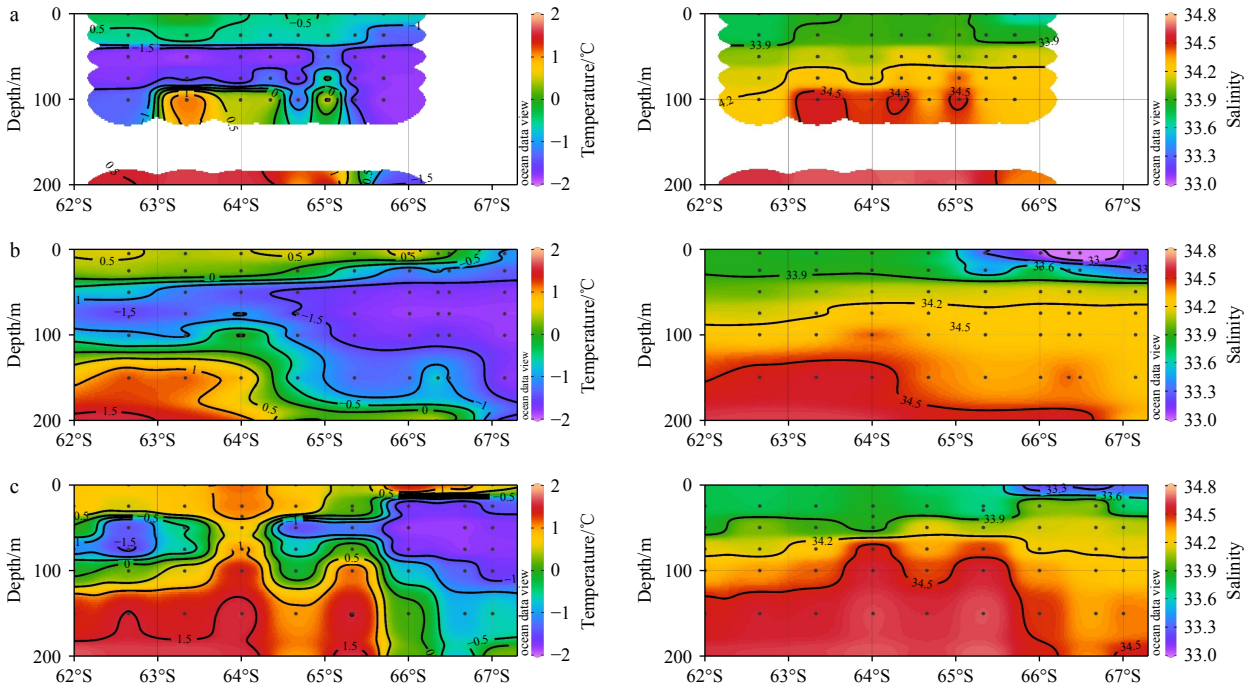


Fig. 2. Vertical distributions of temperature and salinity along 45°E in the Cosmonaut Sea during December 2019 (a), January 2021 (b) and February 2022 (c).

reduced slightly compared to that in January, and deep water with high salinity expanded northward significantly. This similarity in distributions of temperature and salinity suggests the coexistence of at least two water masses characterized by high temperature, high salinity, and low temperature, moderate salinity in the study area during the summer.

3.2 *AOU*

The AOU values are widely used to evaluate water heterotrophy or autotrophy, wherein negative values denote autotrophy and positive values indicate heterotrophy. AOU ranged from –22.9 μmol/kg to 160.4 μmol/kg in the study region during December, with an average value of (53.1 ± 54.5) μmol/kg, and it varied between –40.6 μmol/kg and 162.7 μmol/kg in January, with an average value of (63.4 ± 52.8) μmol/kg; in February, it ranged from –35.3 μmol/kg to 163.3 μmol/kg, averaging (81.5 ± 59.9) μmol/kg (Fig. 3). Overall, vertical distribution of AOU showed strong alignment with salinity patterns, reflecting the unique trophic status of each water mass. Specifically, in December, surface waters shallower than 25 m exhibited negative AOU, indicating autotrophy. In January, the region with negative AOU was confined to south of 64°S but showed a more negative value. By February, the area showing autotrophic reduction was south of 65.5°S, while deep waters with high AOU from mid- and low-latitude spread southward, similar to temperature and salinity trends.

3.3 *Nutrients*

During the austral summer, nitrate concentrations within the study area ranged from 14.0 μmol/L to 35.9 μmol/L [average value: (22.5 ± 6.0) μmol/L] in December, 17.1 μmol/L to 37.8 μmol/L [average value: (29.1 ± 5.0) μmol/L] in January, and 14.8 μmol/L to 34.5 μmol/L [average value: (28.4 ± 4.7) μmol/L] in February (Fig. 4). The nitrate exhibited the highest concentration during January. Vertically, nitrate concentrations increased with depth in December, and the low values (<20 μmol/L) were always observed in the upper 50 m at both ends of the transect. The 20 μmol/L isopleth extended below 100 m at higher latitudes. A tongue of elevated nitrate was observed around 64.3°S, potentially indicative of upwelling. In January, nitrate concentrations were generally above 30 μmol/L below 50 m, while surface waters south of 66°S exhibited concentrations as low as 20 μmol/L. By February, the distribution pattern shifted

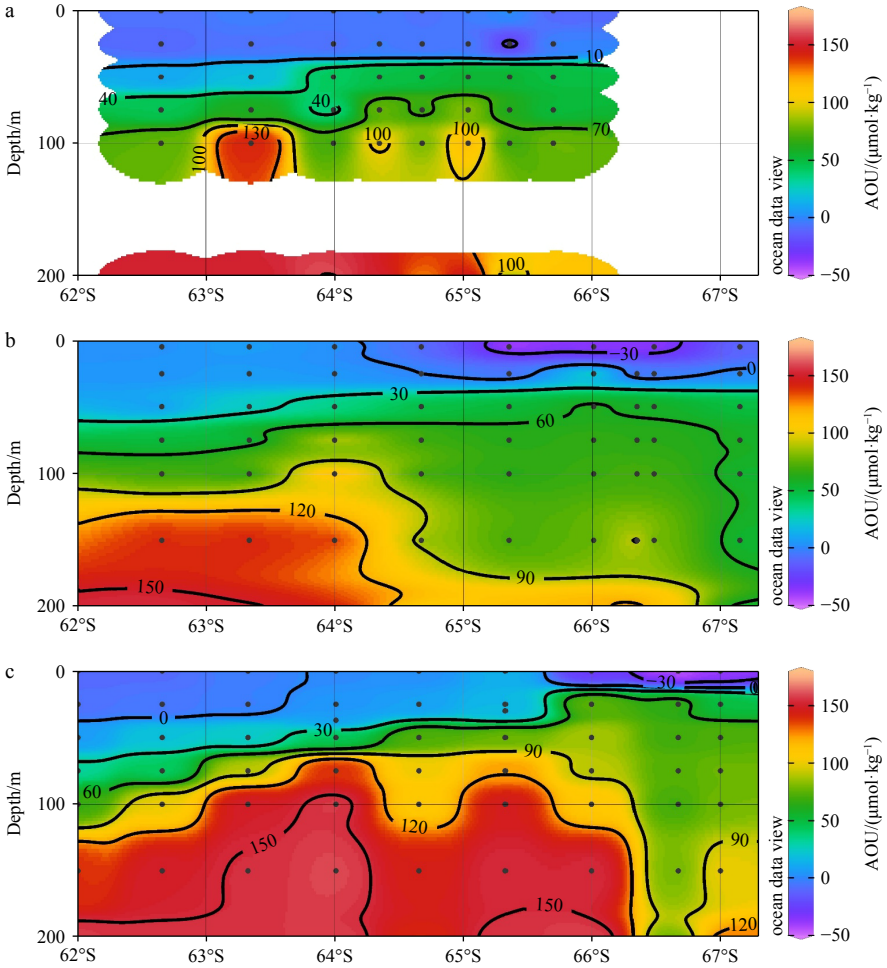


Fig. 3. Vertical distributions of apparent oxygen utilization (AOU) along 45°E in the Cosmonaut Sea during December 2019 (a), January 2021 (b) and February 2022 (c).

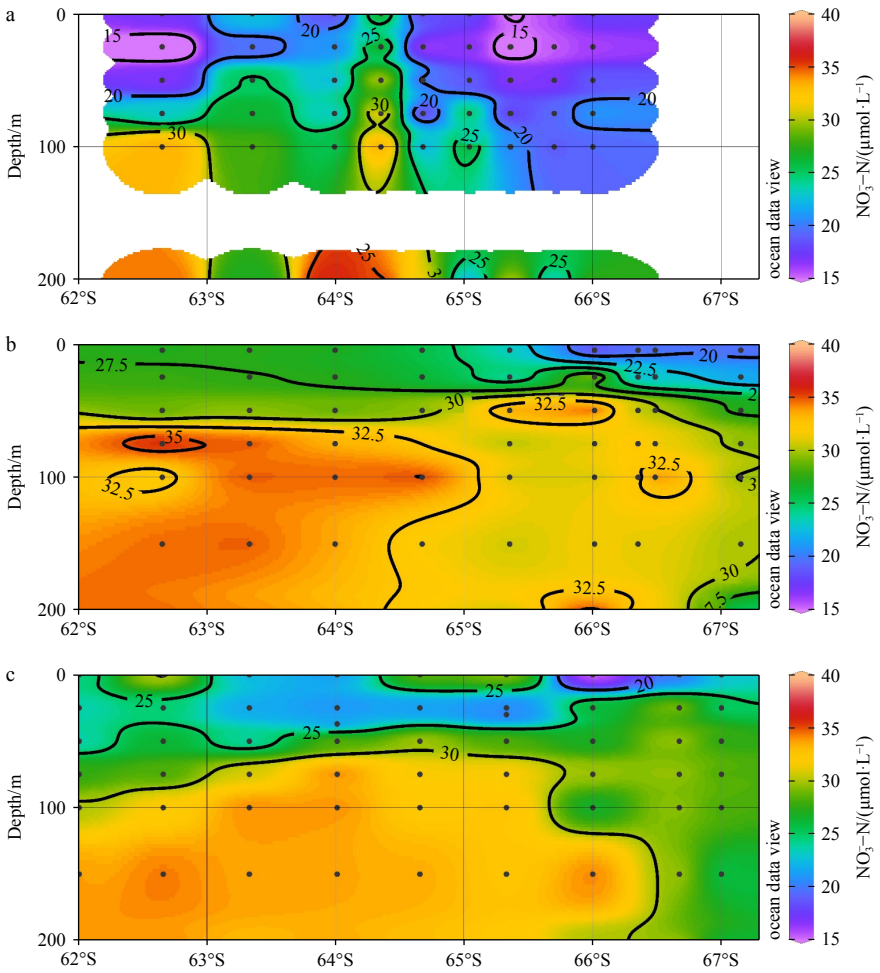


Fig. 4. Vertical distributions of NO_3^--N concentration along 45°E in the Cosmonaut Sea during December 2019 (a), January 2021 (b) and February 2022 (c).

slightly, showing a decrease of approximately 5 μmol/L in the upper 50 m, and the low nitrate waters (<30 μmol/L) spread northward from high latitudes.

Phosphate concentrations ranged from 0.89 μmol/L to 2.48 μmol/L [average value: (1.53 ± 0.37) μmol/L] in December, 0.96 μmol/L to 2.47 μmol/L [average value: (2.01 ± 0.35) μmol/L] in January, and 0.90 μmol/L to 2.67 μmol/L [average value: (2.00 ± 0.40) μmol/L] in February (Fig. 5). The vertical distribution of phosphate largely mirrored that of nitrate. Low phosphate concentrations were observed in the upper 50 m in December, while in January and February, these low concentrations were confined to the upper 25 m south of 65°S. A similar northward expansion of low phosphate waters from high latitudes was also observed.

Silicate concentrations ranged from 21.9 μmol/L to 77.9 μmol/L [average value: (39.9 ± 14.1) μmol/L] in December, 30.8 μmol/L to 82.0 μmol/L [average value: (53.4 ± 12.9) μmol/L] in January, and 14.8 μmol/L to 72.3 μmol/L [average value: (44.7 ± 14.0) μmol/L] in February (Fig. 6). The vertical distribution of silicate generally followed the trends of nitrate and phosphate. However, the lowest silicate concentrations (<20 μmol/L) were observed between 64°S and 65°S in February, whereas the lowest nitrate and phosphate concentrations were located south of 66°S. These distributional differences among the nutrients suggest potentially their distinct utilization patterns.

The nutrient concentrations of winter residual water were also obtained according to its specific identification method. The nitrate, phosphate and silicate in winter water in December were (21.9 ± 3.9) μmol/L, (1.46 ± 0.13) μmol/L, and (36.5 ± 8.5) μmol/L, respectively, which are (31.5 ± 3.1) μmol/L, (2.04 ± 0.08) μmol/L and (52.6 ± 4.4) μmol/L in January and (28.0 ± 1.9) μmol/L, (2.06 ± 0.14) μmol/L, and (41.1 ± 2.8) μmol/L in February. It is obvious that the nutrient levels of winter water are similar to the whole water column.

3.4 *Biogeochemical tracers N*and Si**

$\Delta[N^*]$ values ranged from –6.8 to 5.6 (average value: –2.0 ± 2.2) in December, showing low $\Delta[N^*]$ levels generally (Fig. 7a). For the south of 65°S, $\Delta[N^*]$ values in depths of the upper 100 m remained relatively constant level of around –2.5, while they hovered near 0 northward, exhibiting a relatively homogenous distribution. The largest variations in $\Delta[N^*]$ were observed at 200 m. Compared to that in December, $\Delta[N^*]$ values in January

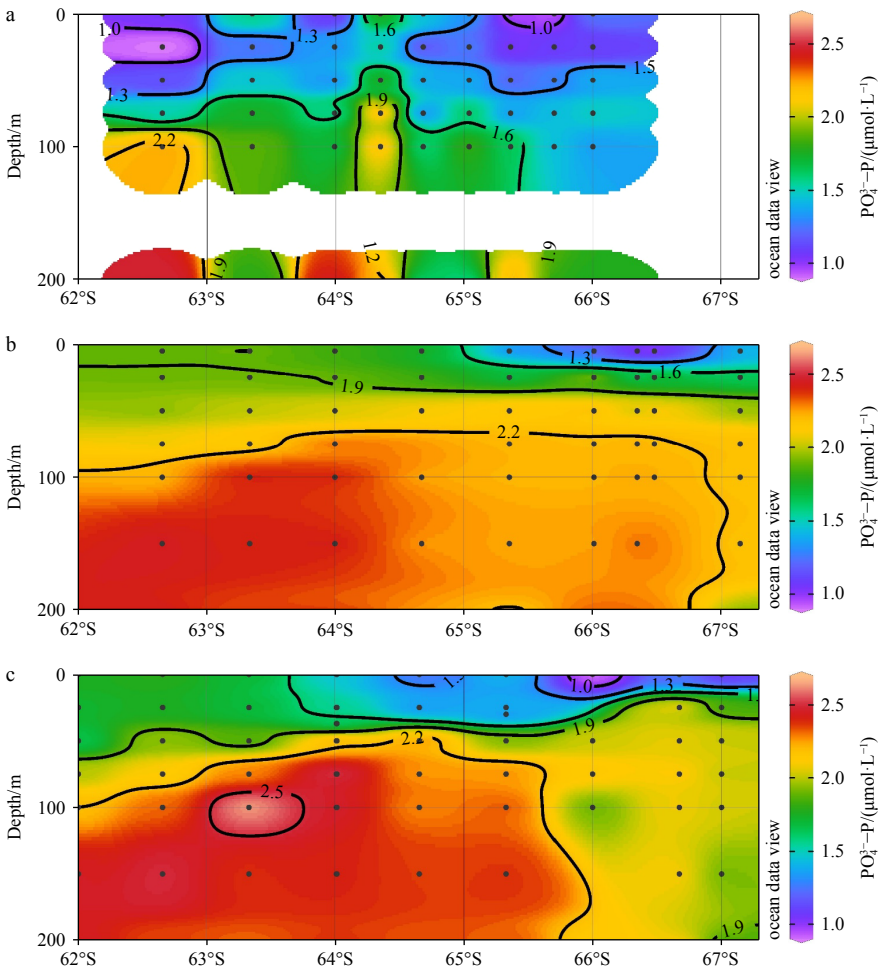


Fig. 5. Vertical distributions of PO_4^{3-}-P concentration along 45°E in the Cosmonaut Sea during December 2019 (a), January 2021 (b) and February 2022 (c).

decreased slightly. Below 75 m south of 64°S, Δ[N*] experienced a reduction of approximately 2.5. By February, the vertical distribution of Δ[N*] changed significantly, characterized by an increase of approximately 5 in the upper 25 m south of 64°S.

Δ[Si*] values in December ranged from 4.5 to 43.3 (average value: 17.4 ± 8.8). The vertical distribution of Δ[Si*] largely mirrored that of Δ[N*], with relatively uniform values of around 15 in the upper 100 m. In contrast to that in December, Δ[Si*] values in January exhibited an increasing trend with depth, showing a pronounced gradient north of 64.5°S and a maximum difference of over 30. Furthermore, the lowest Δ[Si*] values south of 66°S were observed at 25 m or 50 m, rather than at the surface. By February, Δ[Si*] decreased significantly (by about 20) in the upper 25 m, and high Δ[Si*] waters deeper than 100 m appeared to have been transported southward to 66.5°S.

4 Discussion

The Cosmonaut Sea exhibits high biological productivity during the austral summer (Westwood et al., 2010). It was reported that mixed-layer chlorophyll *a* concentrations reached 0.5 mg/m^3 in the region during summer (Demidov et al., 2000), productivity of which also exceeded other frontal zones along the same longitude (Parli et al., 2020). This period is characterized by coupled biogeochemical processes, including glacial meltwater input, ocean currents, nutrient upwelling, and shoaling of the mixed layer. These processes significantly influence nutrient spatiotemporal distribution, composition, and consumption. The factors controlling nutrient dynamics can vary considerably across different periods of summer; hereby, monthly investigation is necessary in the Cosmonaut Sea during summer.

4.1 *Monthly nutrient variations*

This study provided a comprehensive dataset of nutrient concentrations and related parameters for December, January, and February in the Cosmonaut Sea. The nutrient in each month exhibited a distinct distribution pattern. Given the similar distribution of phosphate and nitrate, we focused on nitrate and silicate to explore the monthly variations and their controlling factors to avoid redundancy.

In December, both nitrate and silicate concentrations

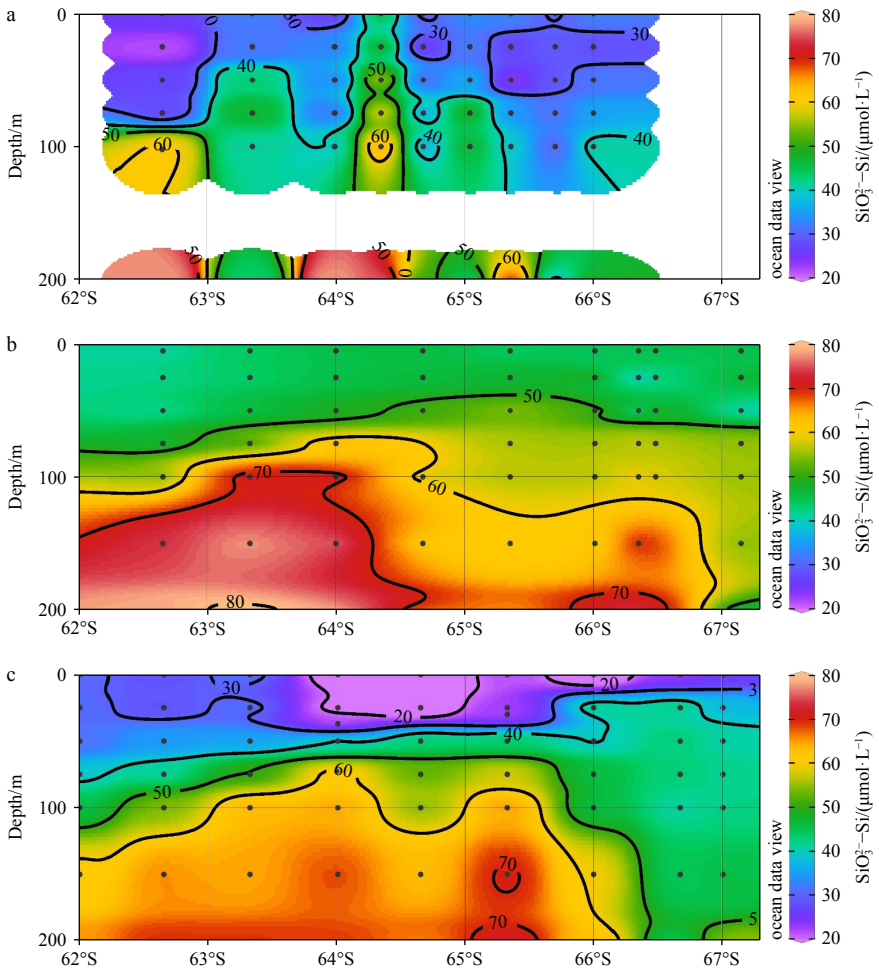


Fig. 6. Vertical distributions of SiO_3^{2-}-Si concentration along 45°E in the Cosmonaut Sea during December 2019 (a), January 2021 (b) and February 2022 (c).

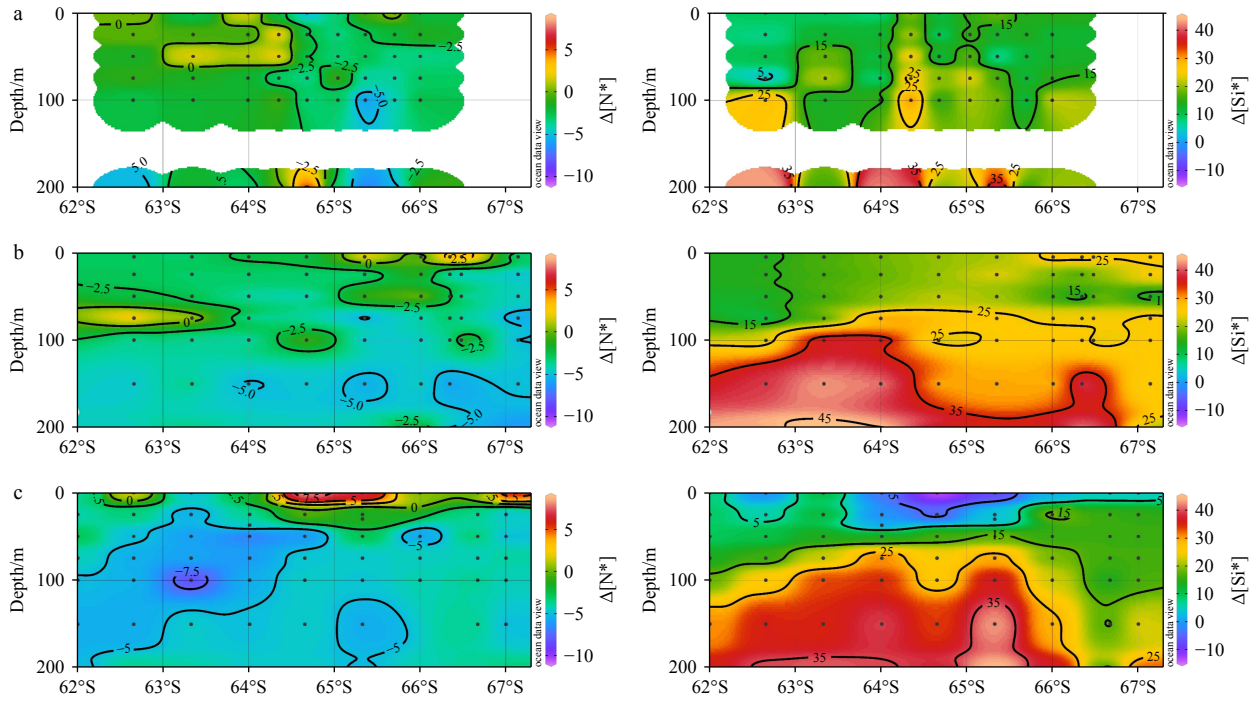


Fig. 7. Vertical distributions of Δ[N*] and Δ[Si*] along 45°E in the Cosmonaut Sea during December 2019 (a), January 2021 (b) and February 2022 (c).

generally increased with depth and were lower in the upper 50 m layer. The vertical profiles of temperature and salinity reveal a sharp change at a depth of about 50 m, indicating the development of a thermocline. This thermocline can provide a stable physical environment conducive to phytoplankton growth, potentially leading to the observed depletion of nitrate and silicate in shallow layers, corroborated by negative AOU values in the same region. Furthermore, the low nitrate zone south of 65.5°S showed low temperature and salinity, suggesting the influence of shelf waters transported by the ASC. We also found that the ice edge was located near 65.5°S during December (Fig. S1). The shelf water with more ice-melting water due to earlier melting would result in dilution of nutrients in the mixed layer of the water column (Parli et al., 2020). In addition, iron (Fe) in the sea ice may be two orders of magnitude higher than that in the underlying seawater (Schoemann et al., 2008). Ice-melting water with high Fe can stimulate phytoplankton growth and further influence the nutrient uptake (van der Merwe et al., 2011), which means that seasonal retreat of the ice edge can induce seasonal phytoplankton bloom and nutrient dynamics.

In January, nitrate concentrations increased substantially compared to those in December, showing relatively homogenous distribution below 50 m. Low nitrate values were confined to the water's upper 50 m south of 65°S. Silicate distribution differed from nitrate slightly, showing a decreasing trend with latitude below 50 m. The temperature-salinity profiles clearly indicate the presence of two distinct water masses: a warm, saline water mass and a cold, moderately saline water mass. The high similarity between nutrient distributions and hydrological properties suggests that water mass mixing significantly influenced nutrient distribution in January. The distribution of AOU, an important indicator of water mass characteristics (Zhang et al., 2024; Parli et al., 2020), further supports this conclusion. The low nitrate zone south of 65.5°S exhibited warm, low salinity characteristics ($T > 0$℃, $S < 33.6$) and more negative AOU, indicating the combined influence of Antarctic Surface Water and biological production. Notably, silicate concentrations did not decrease significantly in this region, suggesting potential preferential uptake of nitrate over silicate by phytoplankton.

Nutrient distributions in February were broadly similar to those in January. However, high-nutrient waters from lower latitudes, characterized by warm, saline conditions and low AOU, continued to intrude southward into the colder, moderately saline waters at higher latitudes. The low nitrate zone expanded northward to 63°S, indicating intensified biological activity. Furthermore, low silicate concentrations were observed within the low nitrate zone. Coupled with the mismatch between nitrate and silicate in the shallow waters south of 65.5°S in January, it suggests that a shift in phytoplankton community composition can significantly alter nutrient stoichiometry.

To further elucidate the influence of biological production and water mass transport on nutrient distributions and stoichiometry, we conducted statistical analyses in detail. Pearson correlation coefficients (Fig. 8) reveal significant positive correlations between nitrate, silicate, and AOU for all three months. Further, the correlation strength (R-values) increased over time from December to February, suggesting a progressively stronger biological control on nutrient dynamics, probably enhanced phytoplankton growth. Biological uptake of nutrients increases with the melting of ice, physical mixing, and increased sunlight (Prend et al., 2019). The above factors, including water temperatures (Fig. 2), ice-melting water with Fe (Fig. S1), and light availability (Garcia et al., 2009), increase with time from December to February.

However, the strong nutrient-AOU correlations may also reflect the influence of water mass mixing, as AOU is a reliable water mass tracer (Guo et al., 2023). Therefore, we also assessed the correlations between salinity and nutrients. The results showed significant positive correla-

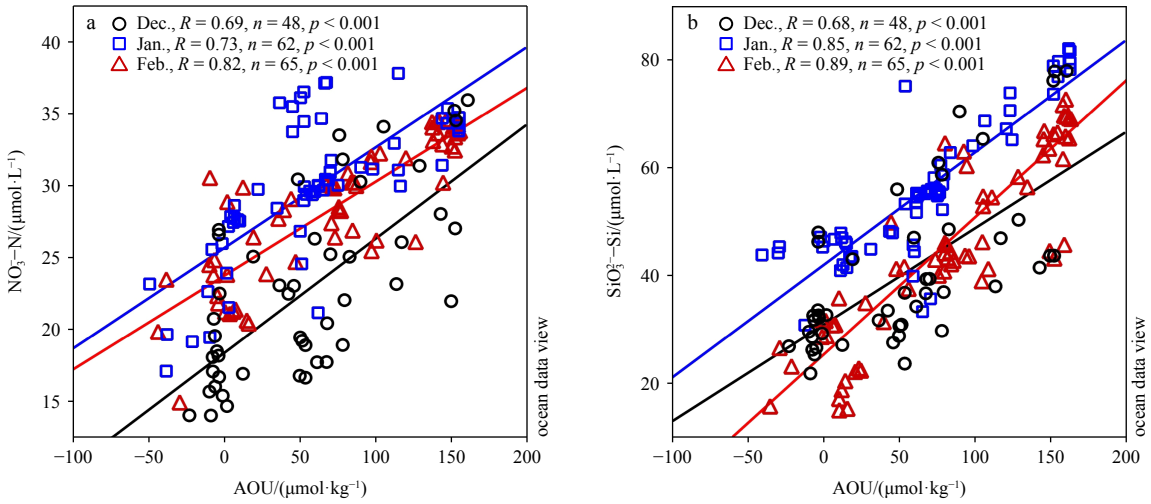


Fig. 8. Pearson correlation between AOU and NO_3^--N (a) or SiO_3^{2-}-Si (b) concentrations during December, January and February in the Cosmonaut Sea.

tions and increasing correlation coefficients over time (Fig. 9), highlighting the importance of water mass transport in regulating nutrient distributions. Analysis of *T-S* relationships (Fig. 9) reveals the presence of CDW, WW, and AASW. The shelf water driven by ASC could be present, but it was hard to identify due to various temperatures and salinity from months. Specifically, the influence of CDW was lowest in January, followed by December, and highest in February, potentially reflecting monthly variations in ocean currents (Moffat et al., 2009). Nutrient-rich CDW upwells and replenishes nutrients in the surface and subsurface layers, which are subsequently consumed by phytoplankton. The interplay of these water masses partly governs nutrient concentrations and spatial distributions.

4.2 *Control factors of Δ[N*] and Δ[Si*]*

Δ[N*] and Δ[Si*] are valuable indicators of the difference between nutrient uptake and Redfield stoichiometry, providing insights into phytoplankton nutrient utilization in the euphotic layer (Sarmiento et al., 2004). In this study, Δ[N*] and Δ[Si*] exhibited substantial monthly variations in the Cosmonaut Sea during austral summer (Fig. 10).

In December, Δ[N*] was relatively homogenous, with values near 0 north of 64.5°S and varying from –5 to –2.5 south of 64.5°S. These values are considerably lower than those reported by Parli et al. (2020) for the polar front. Similar to Δ[N*], Δ[Si*] was also uniform (about 15) throughout the water column, except at a depth of 200 m, consistent with Parli et al. (2020). Δ[N*] values ranged from –2.5 to 0 at the upper 25 m, coinciding with the zone with high phytoplankton productivity (negative AOU). This suggests phytoplankton assimilated nitrate and phosphate by a near-Redfield ratio and consumed slightly less silicate compared to nitrate. South of the Polar Front, phytoplankton species are between diatoms and *P. antarctica* over the austral summer (Giddy et al., 2012). The assimi-

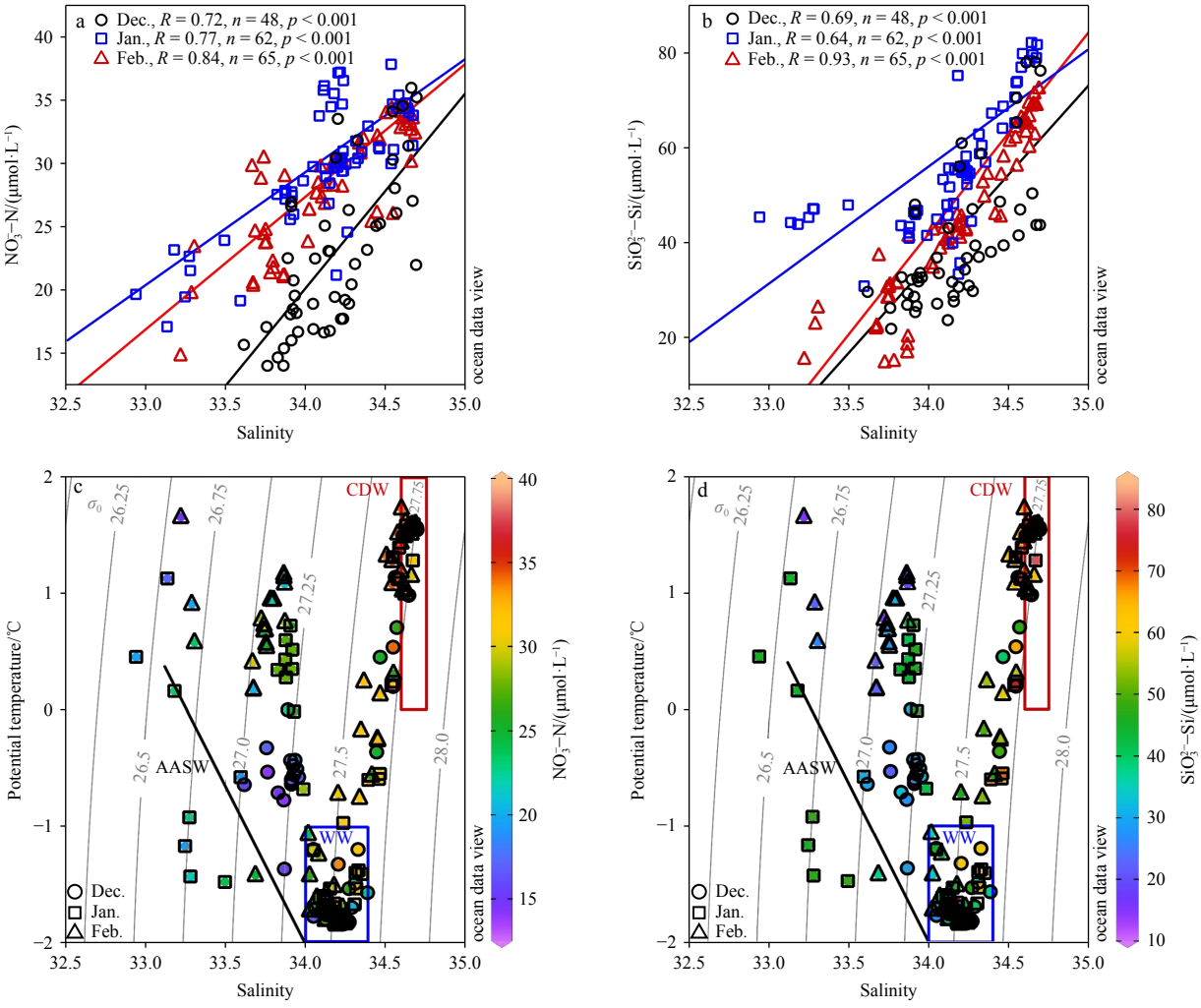


Fig. 9. Pearson Correlation between salinity and NO_3^--N (a) or SiO_3^{2-}-Si (b) concentration during December, January and February in the Cosmonaut Sea, and NO_3^--N (c) or SiO_3^{2-}-Si (d) in different water masses above 200 m depth. The light grey curves represent the contours of potential density anomalies (kg/m^3) referenced to zero pressure. The water masses in the upper 200 m mainly include Antarctic surface water (AASW, black line), winter residual water (WW, blue box) and circumpolar deep water (CDW, red box).

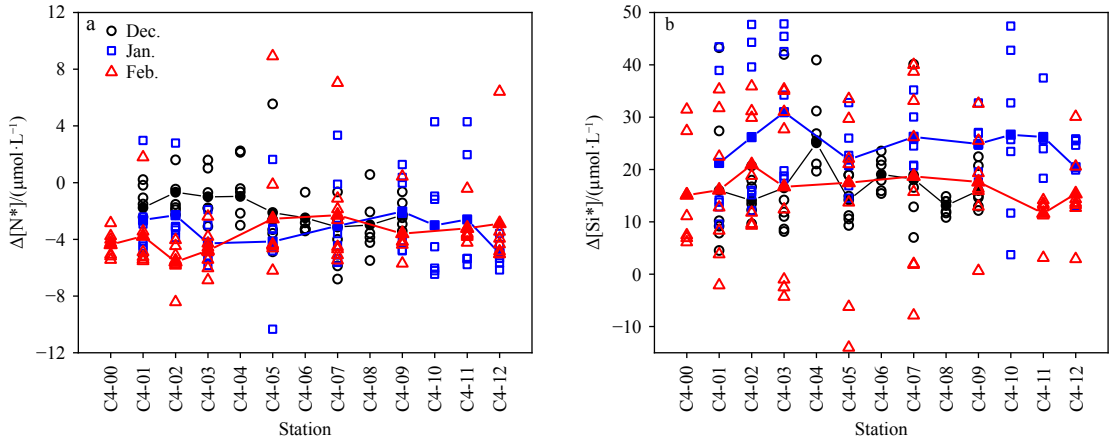


Fig. 10. Δ[N*] (a) and Δ[Si*] (b) variations from stations in all sampling depths along 45°E during December, January and February in the Cosmonaut Sea.

lation ratios of NO_3^--N:PO_4^{3-}-P by these two phytoplanktons are significantly different, which for *P. antarctica* (19.20 ± 0.61) is nearly twice as high as that for diatoms (9.69 ± 0.33) (Arrigo et al., 1999). Moreover, silicon is mainly consumed by diatoms while it is almost not influenced by *P. Antarctica*. Pigment data from the same cruise further indicate that *P. antarctica* dominated the phytoplankton community, contributing 40% of chlorophyll *a* (unpublished data), while diatoms contributed only 23%. This may explain the low Δ[N*] and high Δ[Si*] observed in December.

In January, Δ[N*] levels and distribution remained largely unchanged compared to those in December and showed only a slight decrease at higher latitudes. However, Δ[Si*] exhibited a pronounced increasing gradient with depth, particularly below 100 m. Pigment data indicate that diatom contribution decreased to 17% south of 64°S, while *P. antarctica* increased to 63% (Li et al., 2024). This reduced silicate consumption well corresponds to the elevated Δ[Si*] levels in January, while the near-Redfield N and P uptake by *P. antarctica* explains the Δ[N*] values of near 0.

The study region in February saw significant changes in Δ[N*] and Δ[Si*], primarily in the upper 25 m, showing increasing Δ[N*] and decreasing Δ[Si*]. The low AOU in this region suggests that these changes are also driven by phytoplankton activity. Unlike in December and January, phytoplankton appear to have reduced nitrate consumption (NNU) and increased silicate uptake. We hypothesize that the phytoplankton community shifted towards a siliceous-dominated assemblage over time. Based on unpublished data and the study results in December and January, this siliceous population is likely diatoms. This is supported by CHEMTAX analysis by Wright et al. (2010) for the same region and period, which showed a higher contribution of diatoms to chlorophyll *a* compared to other phytoplankton populations. Giddy et al. (2012) also found a species shift from an early *P. antarctica* bloom to one dominated by diatoms from December to February in the southern and northern Weddell zones. These findings suggest that shifts over time in phytoplankton community structure regulate N and Si utilization during austral summer.

4.3 *Seasonal nutrient depletion*

Seasonal nutrient consumption was calculated using nutrient concentrations of residual winter water (Fig. 11). In December, NNU ranged from 64.1 mmol/m^2 to 213.5 mmol/m^2, with an average value of (134.1 ± 55.0) mmol/m^2. NNU was generally low and slightly higher at higher latitudes. NNU in January was substantially higher, with an average value of (312.2 ± 199.7) mmol/m^2 (2.3 times the average in December), showing high values at both high and low latitudes. NNU in February decreased with an average value of (192.8 ± 100.9) mmol/m^2, showing a marked decline from January, particularly at higher latitudes (over 200 mmol/m^2 reduction).

Phosphate consumption (NPU) in December ranged from 3.6 mmol/m^2 to 19.3 mmol/m^2 [average value: (9.0 ± 6.3) mmol/m^2], mirroring the latitudinal trend of NNU. NPU in January increased with an average value of (18.1 ± 11.1) mmol/m^2, and high values are still at higher latitudes. NPU in February increased slightly with an average value of (21.2 ± 9.4) mmol/m^2, but the highest NNU values at high latitudes corresponded with the lowest NPU values in the study area.

Silicate consumption (NSiU) in December ranged from 108.7 mmol/m^2 to 470.0 mmol/m^2 [average value: (245.8 ± 141.0) mmol/m^2], showing no clear latitudinal trend. Similar to NNU, NSiU in January increased substantially with an average value of (430.0 ± 424.8) mmol/m^2. A high NSiU zone appeared at higher latitudes, mirroring NNU. NSiU in February increased further with an average value of (636.5 ± 419.7) mmol/m^2.

Overall, seasonal nutrient consumption in the Cosmonaut Sea exhibited significant monthly variability, generally increasing over time, except for a decrease in NNU in

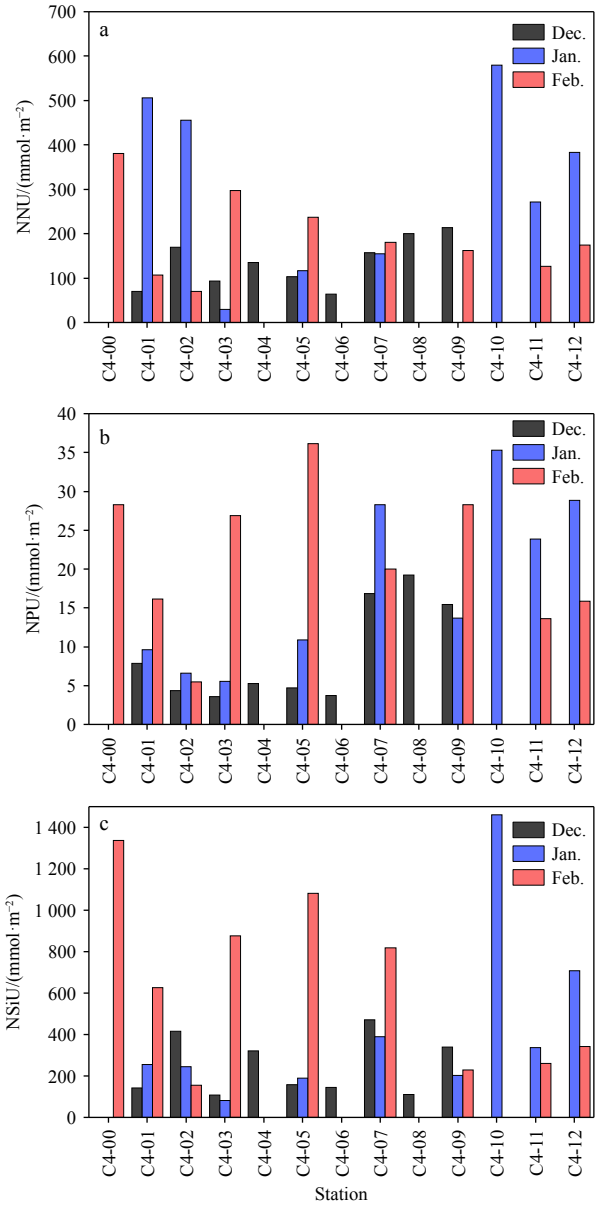


Fig. 11. Variations of seasonal NNU (a), NPU (b) and NSiU (c) with stations along transect of 45°E in the Cosmonaut Sea during December, January and February.

February. This is readily explained by the cumulative nature of nutrient consumption over time in the absence of external nutrient inputs. Spatially, high nutrient consumption in December and January occurred in high-latitude coastal waters, consistent with the distribution of chlorophyll *a* concentrations during these periods (Li et al., 2021; Li et al., 2024). The marginal ice zone during austral summer is characterized by high chlorophyll *a* and primary productivity, leading to substantial nutrient drawdown. However, in February, silicate consumption was disproportionately high compared to nitrate and phosphate, suggesting preferential silicate utilization by phytoplankton, potentially linked to the increased contribution of diatoms to the phytoplankton community in February (Wright et al., 2010). As for NNU in February, its low values are mainly induced by the shallower depth of winter residual water with 50 m, easily inferred by temperature and salinity profiles (Fig. 2).

We compared our estimated nutrient consumption rates with those reported from other seas in the Southern Ocean (Table 1). The results showed that nitrate, phosphate, and silicate consumptions varied considerably among regions. The lowest nitrate and phosphate consumption was observed south of Tasmania in the polar frontal zone, while the highest phosphate and silicate consumption occurred in Marguerite Bay (Serebrennikova et al., 2004). Nutrient consumption in the Cosmonaut Sea was generally lower than that in other regions, comparable to Prydz Bay in January and February (Chen et al., 2017), and similar to the polar frontal zone south of Tasmania (Lourey et al., 2001) in December. Nutrient consumption appears strongly linked to sampling time. Marguerite Bay, with the highest consumption, was sampled in autumn, reflecting the nutrient utilization over the whole summer. In contrast, the polar frontal zone south of Tasmania, Prydz Bay, and the Cosmonaut Sea, sampled in January, only consumed nutrients for one month during summer. Nutrient consumption in February generally exceeded that in December and January for both Prydz Bay and the Cosmonaut Sea. Interestingly, while nitrate and phosphate consumptions in the Cosmonaut Sea in January were lower than those in Prydz Bay during the same period, silicate consumption was higher, suggesting preferential silicate utilization in the Cosmonaut Sea, likely driven by a siliceous-dominated phytoplankton community. These regional differences in nutrient consumption probably reflect variations in seasonal productivity and phytoplankton community structure. We propose that cross-regional comparisons of nutrient depletion estimates should be temporally standardized to account for phenological differences in bloom dynamics.

Based on detailed analysis of nutrient utilization in this study, the pattern of nutrients consumed by phytoplankton can be easily predicted. In early summer, nutrients are mostly consumed by nanophytoplankton such as *P. antarctica* when the sea ice starts to melt and light availability increases. At this time, nitrate is preferentially consumed compared to silicate in the euphotic layer, which probably occurs in coastal waters due to earlier sea ice melting and Fe supply. By mid-summer, phytoplankton blooms consumed amounts of nutrients including nitrate and silicate, under warm and long-time light conditions, together with increasing proportions of lightly silicified diatoms in the phytoplankton population, partly driven by a high grazing index (Pillai et al., 2018). In later summer, nutrients are further utilized and show overconsumption of silicate relative to nitrate when diatoms gradually dominate instead of *P. antarctica*. Thus, it can be seen that the nutrient cycle is strongly influenced by marine phytoplankton and vice versa. A high temporal resolution survey is necessary to understand the interacting

Table 1. Comparison of seasonal depletion of nutrients in different regions

Study area	Nitrate depletion NNU/(mmol·m^{-2})	Phosphate depletion NPU/(mmol·m^{-2})	Silicate depletion NSiU/(mmol·m^{-2})	Sampling time
Ross Sea	460.0	20.0	490.0	autumn 1997
(Sweeney et al., 2000)				
Marguerite Bay	540.0	40.0	2 000.0	autumn 2001
(Serebrennikova et al., 2004)	410.0	40.0	1 600.0	autumn 2002
Tasmania Front Zone	150.0	12.0	–	Jan. 1995
(Lourey et al., 2001)	170.0	13.0	–	Jan. 1994
	170.0	15.0	–	Jan. 1995
Prydz Bay	445.4	28.1	528.7	Feb. 2009
(Chen et al., 2017)	366.0	25.3	382.3	Jan. 2011
	345.8	20.4	571.1	Feb. 2013
Cosmonaut Sea (this study)	134.1	9.0	245.8	Dec. 2019
	312.2	18.1	430.0	Jan. 2021
	192.8	21.2	636.5	Feb. 2022

Note: − represents no data.

mechanism between nutrient and phytoplankton populations, including their controlling factors.

5 Conclusions

The nutrient distribution varied significantly from December to February during austral summer in the Cosmonaut Sea, most of which can be attributed to phytoplankton productivity and water mass. The water at high latitude always kept a low concentration caused by primary production, speculated from low AOU. The shelf water with rich microelements stimulated the bloom of phytoplankton near the sea ice zone. The distributions of biogeochemical tracers ($\Delta[N^*]$ and $\Delta[Si^*]$) further indicated that nutrient utilization was largely influenced by the phytoplankton community in the euphotic layer. Differential phytoplankton uptake of silicate and nitrate leads to the $\Delta[N^*]$ and $\Delta[Si^*]$ variabilities, reflecting the increase in diatom abundance compared to the other phytoplankton, such as *P. antarctica*, from December to February. The nutrient depletion also showed the large increasing silicate consumption from December to February, corresponding to increasing $\Delta[Si^*]$ value. Our estimated nutrient depletion was similar to that of Prydz Bay at the same month and lower than that in Marguerite Bay due to different sampling times. Of course, nutrient depletion was directly related to phytoplankton productivity and phytoplankton community. We recommend that the comparisons of estimated nutrient depletion be better conducted during the same period in order to accurately evaluate the influence of phytoplankton productivity and phytoplankton community. Though there are some uncertainties about the above conclusions, mainly due to using a single transect from three different years' surveys to reflect the regional condition and seasonal variability, the monthly variability of nutrients is still credible, inferred from sea ice monthly change. In subsequent research, the datasets from the literature and historical expeditions in the Cosmonaut Sea during summer will be collected and normalized to reduce the uncertainty of study results.

Acknowledgements

We would like to thank the crews of the R/V *Xuelong 2* for their assistance with sample collection and the hydrological data provided by the Physical Ocean Group.

References

Arrigo K R. 1999. Phytoplankton community structure and the drawdown of nutrients and CO_2 in the Southern Ocean. Science, 283(5400): 365–367, doi: 10.1126/science.283.5400.365

Buma A G J, De Baar H J W, Nolting R F, et al. 1991. Metal enrichment experiments in the Weddell-Scotia Seas: effects of iron and manganese on various plankton communities. Limnology and Oceanography, 36(8): 1865–1878, doi: 10.4319/lo.1991.36.8.1865

Burkill P H, Edwards E S, Sleight M A. 1995. Microzooplankton and their role in controlling phytoplankton growth in the marginal ice zone of the Bellingshausen Sea. Deep Sea Research Part Ⅱ: Topical Studies in Oceanography, 42: 1277–1290, doi: 10.1016/0967-0645(95)00060-4

Chen Jiyu, Han Zhengbing, Hu Chuanyu, et al. 2017. Distribution and seasonal depletion of nutrients in Prydz Bay, Antarctica. Chinese Journal of Polar Research (in Chinese), 20(3): 327–337

Demidov A B, Vedernikov V I, Sheberstov S V. 2007. Spatiotemporal variability of chlorophyll *a* in the Atlantic and Indian sectors of the Southern Ocean during February–April of 2000 according to satellite and expeditionary data. Oceanology, 47(4): 507–518, doi: 10.1134/S0001437007040 08X

Ding Yufei, Zhu Changfeng, Zhang Cai, et al. 2022. Distributions of dissolved oxygen and apparent oxygen utilization in the Cosmonaut Sea and Amundsen Sea in austral sum-

mer 2022. Advances in Polar Science, 35(3): 327–369

Fan Lingfang, Chen Min, Yang Zifei, et al. 2024. Alleviated photoinhibition on nitrification in the Indian Sector of the Southern Ocean. Acta Oceanologica Sinica, 43: 52–69, doi: 10.1007/s13131-024-2379-7

Gandhi N, Ramesh R, Laskar A H, et al. 2012. Zonal variability in primary production and nitrogen uptake rates in the southwestern Indian Ocean and the Southern Ocean. Deep-Sea Research Part Ⅰ, 67: 32–43, doi: 10.1016/j.dsr.2012.05.003

Garcia N S, Sedwick P N, DiTullio G R, et al. 2009. Influence of irradiance and iron on the growth of colonial *Phaeocystis antarctica*: implications for seasonal bloom dynamics in the Ross Sea, Antarctica. Aquatic Microbial Ecology, 57(2): 203–220.

Giddy I S, Swart S, Tagliabue A. 2012. Drivers of non-Redfield nutrient utilization in the Atlantic sector of the Southern Ocean. Geophysical Research Letters, 39(L17604): 1–6

Grasshoff K, 1983. Determination of Oxygen. Second, Revised and Extended Edition. Germany: Verlag Chemie, 61–72

Gruber N, Dominic C, Brendan R C. 2019. The oceanic sink for anthropogenic CO_2 from 1994 to 2007. Science, 363: 1193–1199, doi: 10.1126/science.aau5153

Gruber N, Landschützer P, Lovenduski N S. 2019. The variable Southern Ocean carbon sink. Annual review of marine science, 11: 159–186, doi: 10.1146/annurev-marine-121916-063407

Guo Jiaying, Yang Xufeng, Zhao Jun, et al. 2023. Distributions of dissolved oxygen and apparent oxygen utilization in the Cosmonaut Sea and Amundsen Sea in austral summer 2021. Advances in Polar Science, 34(4): 272–303

Hao Guanghua, Shen Hui, Wang Anliang, et al. 2025. Temporal dynamics of open ocean polynyas influenced by sea ice and climatic impacts in the West Cosmonaut Sea. Journal of Geophysical Research: Oceans, 130(1): e2024JC021815, doi: 10.1029/2024JC021815

Holm-Hansen O, Amos A S N, Nelson Silva, et al. 1994. *In situ* evidence for a nutrient limitation of phytoplankton growth in pelagic Antarctic waters. Antarctic Science, 6(3): 315–324, doi: 10.1017/S0954102094000489

Huang Wenhao, Yang Xufeng, Zhao Jun, et al. 2022. Dissolved nutrient distributions in the Antarctic Cosmonaut Sea in austral summer 2021. Advances in Polar Science, 33(3): 267–290, doi: 10.13679/j.advps.2022.0099

Hutchins D A, Bruland K W. 1998. Iron-limited diatom growth and Si: N uptake ratios in a coastal upwelling regime. Nature, 393(6685): 561–564, doi: 10.1038/31203

Karl D M, Tilbrook B D, Tien G. 1991. Seasonal coupling of organic matter production and particle flux in the western Bransfield Strait, Antarctica. Deep Sea Research Part A. Oceanographic Research Papers, 38(8−9): 1097–1126

Li Qingmiao, Xiao Wenshen, Wang Rujian, et al. 2021. Diatom based reconstruction of climate evolution through the Last Glacial Maximum to Holocene in the Cosmonaut Sea, East Antarctica. Deep Sea Research Part Ⅱ: Topical Studies in Oceanography, 194: 104960, doi: 10.1016/j.dsr2.2021.104960

Li Yuhong, Zhao Jun, Li Dong, et al. 2024. Factors controlling the phytoplankton crops, taxonomic composition, and particulate organic carbon stocks in the Cosmonaut Sea, East Antarctica. Journal of Oceanology and Limnology, 42(6): 1895–1908, doi: 10.1007/s00343-024-3198-6

Lourey M J, Trull T W. 2001. Seasonal nutrient depletion and carbon export in the Subantarctic and Polar Frontal Zones of the Southern Ocean south of Australia. Journal of Geophysical Research: Oceans, 106(C12): 31463–31487, doi: 10.1029/2000JC000287

Martiny A C, Pham C T A, Primeau F W, et al. 2013. Strong latitudinal patterns in the elemental ratios of marine plankton and organic matter. Nature Geoscience, 6(4): 279–283, doi: 10.1038/ngeo1757

Meijers A J S, Klocker A, Bindoff N L, et al. 2010. The circulation and water masses of the Antarctic shelf and continental slope between 30 and 80°E. Deep Sea Research Part Ⅱ: Topical Studies in Oceanography, 57(9−10): 723–737, doi: 10.1016/j.dsr2.2009.04.019

Mitchell B G, Brody E A, Holm-Hansen O, et al. 1991. Light limitation of phytoplankton biomass and macronutrient utilization in the Southern Ocean. Limnology and Oceanography, 36(8): 1662–1677, doi: 10.4319/lo.1991.36.8.1662

Moffat C, Owens B, Beardsley R C. 2009. On the characteristics of Circumpolar Deep Water intrusions to the west Antarctic Peninsula Continental Shelf. Journal of Geophysical Research: Oceans, 114(C05017): 1–16

Nelson D M, Smith W O Jr. 1991. Sverdrup revisited: critical depths, maximum chlorophyll levels, and the control of Southern Ocean productivity by the irradiance-mixing regime. Limnology and Oceanography, 36(8): 1650–1661, doi: 10.4319/lo.1991.36.8.1650

Orsi A H, Whitworth III T W, Nowlin Jr W D. 1995. On the meridional extent and fronts of the Antarctic Circumpolar Current. Deep Sea Research Part Ⅰ: Oceanographic Research Papers, 42(5): 641–673, doi: 10.1016/0967-0637(95)00021-W

Parli B V, Dessai D R G, Anilkumar N, et al. 2020. Meridional variations in N^* and Si^* along 57°30′E and 47°E transects in the Indian sector of the Southern Ocean during austral summer 2011. Deep Sea Research Part Ⅱ: Topical Studies in Oceanography, 178: 104846, doi: 10.1016/j.dsr2.2020.104846

Pillai H U K, Anilkumar N, Achuthankutty C T, et al. 2018. Planktonic food web structure at SSTF and PF in the Indian sector of the Southern Ocean during austral summer 2011. Polar Research, 37(1): 1495545, doi: 10.1080/17518369.2018.1495545

Prend J C, Gille S T, Talley L D, et al. 2019. Physical Drivers of Phytoplankton Bloom Initiation in the Southern Ocean's Scotia Sea. Journal of Geophysical Research: Oceans, 124(8): 5611–5626, doi: 10.1029/2019JC015162

Qi Qianqian, Hao Qiang, Yang Guang, et al. 2024. Diverse im-

pacts of sea ice and ice shelf melting on phytoplankton communities in the Cosmonaut Sea, East Antarctica. Environmental Research Letters, 20(2025): 014003

Quigg A, Finkel Z V, Irwin A J, et al. 2003. The evolutionary inheritance of elemental stoichiometry in marine phytoplankton. Nature, 425: 291–294, doi: 10.1038/nature01953

Rubin S I, Takahashi T, Chipman D W, et al. 1998. Primary productivity and nutrient utilization ratios in the Pacific sector of the Southern Ocean based on seasonal changes in seawater chemistry. Deep Sea Research Part Ⅰ: Oceanographic Research Papers, 45(8): 1211–1234, doi: 10.1016/S0967-0637(98)00021-1

Sarmiento J L, Gruber N, Brzezinski M A, et al. 2004. High-latitude controls of thermocline nutrients and low latitude biological productivity. Nature, 42: 56–60

Schoemann V S, Jong J T M D, Lannuzel D, et al. 2008. Microbiological control on the cycling of Fe and its isotopes in Antarctic sea ice. Geochmica Et Cosmochimica Acta, 72(12): A837

Serebrennikova Y M, Fanning K A. 2004. Nutrients in the Southern Ocean GLOBEC region: variations, water circulation, and cycling. Deep Sea Research Part Ⅱ: Topical Studies in Oceanography, 51(17–19): 1981–2002, doi: 10.1016/j.dsr2.2004.07.023

Sullivan C W, Arrigo K R, Mcclain C R, et al. 1993. Distributions of phytoplankton blooms in the Southern Ocean. Science, 262(5141): 1832–1837, doi: 10.1126/science.262.5141.1832

Sweeney C, Hansell D A, Carlson C A, et al. 2000. Biogeochemical regimes, net community production and carbon export in the Ross Sea, Antarctica. Deep Sea Research Part Ⅱ: Topical Studies in Oceanography, 47(15−16): 3369–3394, doi: 10.1016/S0967-0645(00)00072-2

Takeda S. 1998. Influence of iron availability on nutrient consumption ratio of diatoms in oceanic waters. Nature, 393(6687): 774–777, doi: 10.1038/31674

Timmermans K R, Wagt B V D, Baar H J W D. 2004. Growth rates, half-saturation constants, and silicate, nitrate, and phosphate depletion in relation to iron availability of four large, open-ocean diatoms from the Southern Ocean. Limnology and Oceanography, 49(6): 2141–2151, doi: 10.4319/lo.2004.49.6.2141

Van Der Merwe P, Lannuzel D, Bowie A R, et al. 2011. High temporal resolution observations of spring fast ice melt and seawater iron enrichment in East Antarctica. Journal of Geophysical Research: Biogeosciences, 116(G03017): 1–18

Westwood K J, Griffiths F B, Meiners K M, et al. 2006. Primary productivity off the Antarctic coast from 30°–80°E; BROKE-West survey. Deep-Sea Research Part Ⅱ, 2010, 57(9–10): 794–814

Williams G D, Nicol S, Aoki S, et al. 2010. Surface oceanography of BROKE-West, along the Antarctic Margin of the South-West Indian Ocean (30–80°E). Deep-Sea Research Ⅱ, 57(9–10): 738–757, doi: 10.1016/j.dsr2.2009.04.020

Wright S W, Enden R L V D, Pearce I, et al. 2010. Phytoplankton community structure and stocks in the Southern Ocean (30–80°E) determined by CHEMTAX analysis of HPLC pigment signatures. Deep-Sea Research Part Ⅱ, 2010, 57(9−10): 758–778

Zhang Rui, Blain S, Baudet C, et al. 2024. Tagging of water masses with covariance of trace metals and prokaryotic taxa in the Southern Ocean. Limnology and Oceanography Letters, 9(6): 776–784, doi: 10.1002/lol2.10429

Supplementary information:

Fig. S1. Ice concentrations in the Cosmonaut Sea on 24 December 2019 (a), 22 January 2021 (b) and 2 February 2022 (c), respectively.

Table S1. Nutrients and other related parameters for stations along 45°E transect in the Cosmonaut Sea during the three cruises.

The supplementary information is available online at https://doi.org/11.1007/s13131-025-2480-6 and http://www.aosocean.com/. The supplementary information is published as submitted, without typesetting or editing. The responsibility for scientific accuracy and content remains entirely with the authors.